JOURNAL OF VIROLOGY, Feb. 2002, p. 1415–1421 Vol. 76, No. 3
0022-538X/02/$04.00+0 DOI: 10.1128/JVI.76.3.1415–1421.2002

The g5R (D250) Gene of African Swine Fever Virus Encodes a Nudix Hydrolase That Preferentially Degrades Diphosphoinositol Polyphosphates

Jared L. Cartwright,[1] Stephen T. Safrany,[2] Linda K. Dixon,[3] Edward Darzynkiewicz,[4] Janusz Stepinski,[4] Richard Burke,[1] and Alexander G. McLennan[1]*

School of Biological Sciences, University of Liverpool, Liverpool L69 7ZB,[1] School of Life Sciences, University of Dundee, Dundee DD1 5EH,[2] and Institute for Animal Health, Pirbright GU24 0NF,[3] United Kingdom, and Department of Biophysics, Institute of Experimental Physics, University of Warsaw, 02-089 Warsaw, Poland[4]

Received 9 August 2001/Accepted 5 September 2001

The African swine fever virus (ASFV) g5R gene encodes a protein containing a Nudix hydrolase motif which in terms of sequence appears most closely related to the mammalian diadenosine tetraphosphate (Ap_4A) hydrolases. However, purified recombinant g5R protein (g5Rp) showed a much wider range of nucleotide substrate specificity compared to eukaryotic Ap_4A hydrolases, having highest activity with GTP, followed by adenosine 5′-pentaphosphate (p_5A) and dGTP. Diadenosine and diguanosine nucleotides were substrates, but the enzyme showed no activity with cap analogues such as $7mGp_3A$. In common with eukaryotic diadenosine hexaphosphate (Ap_6A) hydrolases, which prefer higher-order polyphosphates as substrates, g5Rp also hydrolyzes the diphosphoinositol polyphosphates PP-$InsP_5$ and $[PP]_2$-$InsP_4$. A comparison of the kinetics of substrate utilization showed that the k_{cat}/K_m ratio for PP-$InsP_5$ is 60-fold higher than that for GTP, which allows classification of g5R as a novel diphosphoinositol polyphosphate phosphohydrolase (DIPP). Unlike mammalian DIPP, g5Rp appeared to preferentially remove the 5-β-phosphate from both PP-$InsP_5$ and $[PP]_2$-$InsP_4$. ASFV infection led to a reduction in the levels of PP-$InsP_5$, ATP and GTP by ca. 50% at late times postinfection. The measured intracellular concentrations of these compounds were comparable to the respective K_m values of g5Rp, suggesting that one or all of these may be substrates for g5Rp during ASFV infection. Transfection of ASFV-infected Vero cells with a plasmid encoding epitope-tagged g5Rp suggested localization of this protein in the rough endoplasmic reticulum. These results suggest a possible role for g5Rp in regulating a stage of viral morphogenesis involving diphosphoinositol polyphosphate-mediated membrane trafficking.

The Nudix hydrolases are members of a phylogenetically widespread enzyme family that hydrolyze predominantly the diphosphate (pyrophosphate) linkage in a variety of nucleoside triphosphates, dinucleoside polyphosphates, nucleotide sugars and nucleotide cofactors having the general structure of a nucleoside diphosphate linked to another moiety, X (1, 15). They all possess the Nudix sequence signature motif Gx_5Ex_5 [UA]xREx_2EExGU (where U is an aliphatic hydrophobic amino acid), formerly known as the MutT motif (1, 14). It is likely that these enzymes play the dual roles of removing potentially toxic nucleotides and nucleotide metabolites (e.g., oxidized nucleotides, ADP-ribose) from the cellular pools and of adjusting the levels of nucleotide cofactors and messengers in response to metabolic pressures and requirements (1). Gene sequences have been determined for a large number of Nudix hydrolases from archaea, eubacteria, animals, plants, and fungi, and many of the gene products have also been isolated and studied (4, 10, 16, 27). Among the most intriguing of these are the Ap_6A hydrolases (also known as the DIPP subfamily), which hydrolyze highly phosphorylated dinucleoside polyphosphates such as diadenosine 5′,5‴-P^1,P^5-pentaphosphate (Ap_5A) and diadenosine 5′,5‴-P^1,P^6-hexaphosphate (Ap_6A) but which appear to be most active with the structurally unrelated nonnucleotide substrates, diphosphoinositol pentakisphosphate (PP-$InsP_5$) and bisdiphosphoinositol tetrakisphosphate ($[PP]_2$-$InsP_4$) (2, 5, 13, 19).

Genes potentially encoding Nudix hydrolases are also present in the genomes of some double-stranded animal DNA viruses. Vaccinia virus has two Nudix genes, D9 and D10, which share 21% sequence identity and 33% sequence similarity, and several other members of the *Poxviridae* have pairs of related genes. So far, a single Nudix gene has been found in the genomes of the iridoviruses *Chilo Iridescent Virus* and *Lymphocystis Disease Virus* and in the sole representative of the *Asfarviridae*, *African Swine Fever Virus* (ASFV). Recently, the essential vaccinia virus D10 gene was shown to inhibit cap-dependent translation, but not cap-independent translation, when overexpressed in mammalian cells, and a role in the metabolism of cap-related structures, which have similarities to dinucleoside polyphosphates, was suggested (24). In this study, we describe for the first time the cloning and characterization of a 30-kDa viral Nudix hydrolase, the ASFV g5R (also known as D250) protein (g5Rp) and show that it hydrolyzes a range of nucleoside and dinucleoside polyphosphates but has only low activity toward cap analogue nucleotides containing 7-methylguanine. However, like the DIPP subfamily, g5Rp exhibits the greatest hydrolytic efficiency with diphosphoinositol polyphosphates.

* Corresponding author. Mailing address: School of Biological Sciences, Life Sciences Building, University of Liverpool, P.O. Box 147, Liverpool L69 7ZB, United Kingdom. Phone: 44-151-794-4369. Fax: 44-151-794-4349. E-mail: agmclen@liv.ac.uk.

MATERIALS AND METHODS

Materials. The pST8 plasmid containing the cloned ASFV g5R open reading frame (ORF) was kindly donated by S. R. F. Twigg (26). *Pfu* DNA polymerase was from Stratagene. All mononucleotides and diadenosine and diguanosine polyphosphates were from Sigma, except p_5A, which was synthesized by using recombinant LysU lysyl-tRNA synthetase and tetrapolyphosphate (5). Ap_2G, Ap_3G, Ap_4G, Ap_5G, and Ap_6G were kindly provided by H. Schlüter (Freie Universität Berlin). 7-Methylated cap analogues were synthesized as previously described (8, 25). [^{3}H]inositol was from Amersham Pharmacia Biotech. PP-[^{3}H]$InsP_5$ and [PP] $_2$-[^{3}H]$InsP_4$ were prepared from incomplete phosphorylation of [^{3}H]inositol hexakisphosphate ($InsP_6$; NEN) and purified as described previously (19). Unlabeled PP-$InsP_5$ was a kind gift from J. R. Falck (University of Texas Southwestern Medical Center, Dallas).

Cloning of the g5R ORF. The g5R ORF was amplified from the plasmid pST8 by using the PCR and an upstream T7 20-mer primer (TAATACGACTCACT ATAGGG) and a downstream 37-mer *Bam*HI primer (CACCCAGGATCCCA CCTAATGCTTATATCGTAAATAG). After amplification with *Pfu* DNA polymerase, the DNA was recovered by phenol-chloroform extraction and digested with *Nde*I and *Bam*HI, and the gel-purified restriction fragment was ligated into the *Nde*I and *Bam*HI sites of the pET15b expression vector (Novagen) to give the construct pET-g5R, in which the g5R ORF is located downstream of a His tag sequence. The plasmid was used to transform *Escherichia coli* XL1-Blue cells for propagation.

Protein expression in *E. coli* and purification. *E. coli* strain BL21(DE3) was transformed with pET-g5R, and expression was induced for 3 h with 0.5 mM isopropyl-1-thio-β-D-galactopyranoside as previously described (3). The induced cells (2.5 g) were harvested, washed, and resuspended in 50 ml of breakage buffer (50 mM Tris-HCl, pH 8.0, 0.1 M NaCl). The cell suspension was sonicated, and the soluble cell lysate was recovered by centrifugation at 20,000 × *g* for 25 min. The supernatant was applied at 1 ml/min to a 15-by-50-mm column of Ni^{2+}-nitrilotriacetic acid (NTA)-agarose (Sigma) equilibrated with 37.5 mM Tris-HCl (pH 8.0)–225 mM NaCl. After elution of the unbound protein, a 30-min gradient of 0 to 50 mM histidine in 50 mM Tris-HCl (pH 8.0)–300 mM NaCl was applied at 1 ml/min. Fractions (1 ml) were analyzed by sodium dodecyl sulfate-polyacrylamide gel electrophoresis (SDS-PAGE), and those containing pure g5R protein (g5Rp) were pooled and concentrated by ultrafiltration (Amicon).

Assays and product identification. Unless otherwise stated, nucleotide hydrolysis by g5Rp was assayed and reaction products identified by high-performance ion-exchange chromatography as follows. Assay mixtures (100 μl) containing 50 mM 1,3-bis[Tris(hydroxymethyl)-methylamino]-propane (pH 9.5), 10 mM $MgCl_2$, substrate (various concentrations), and 0.84 μg of g5Rp were incubated for 10 min at 37°C, and 90 μl was applied to a 1-ml Resource-Q column (Pharmacia) at 2 ml/min in 35 mM NH_4HCO_3 (pH 9.6). The elution system was as follows: buffer A (H_2O), buffer B (0.7 M NH_4HCO_3, pH 9.6), and gradient of 5 to 100% buffer B over 10 min. Peaks were identified with the aid of standards and quantified by area integration. Diphosphoinositol polyphosphate hydrolysis by g5Rp was assayed as described previously for DIPP (19) in assay mixtures (500 μl) containing 50 mM HEPES (pH 7.2), 50 mM KCl, 4 mM CHAPS {3-[(3-cholamidopropyl)-dimethylammonio]-1-propanesulfonate}, 0.05 mg of bovine serum albumin/ml, 2 mM $MgSO_4$, and 1 mM Na_2EDTA at 37°C. At appropriate times, aliquots were quenched, neutralized, and subsequently analyzed by high-pressure liquid chromatography (HPLC) as previously described (20).

Determination of substrate metabolism in ASFV-infected cells. Vero cells were incubated in inositol-free Dulbecco modified Eagle medium containing 10% dialyzed fetal calf serum for 4 days and then for a further 3 days in 24-well plates in the same medium containing 200 μCi of [^{3}H]inositol/ml. Cells were infected with the ASFV BA71V isolate at a multiplicity of infection of 3 to 5 in the presence of [^{3}H]inositol for either 4 h or 20 h. Cells were harvested in 50 μl of 0.6 M perchloric acid and then 35 μl of 1 M K_2CO_3–5 mM EDTA was added. Precipitates were removed by centrifugation and supernatants diluted in 1 mM EDTA and analyzed by HPLC as previously described (20). GTP was determined by in-line monitoring of absorbance (A_{260}) of extracts during the HPLC analysis; standards were used to determine the elution time and resolution from other nucleotides. ATP was determined in samples of unfractionated extracts by using a luciferase-based ATP assay kit (Calbiochem-Novabiochem).

Construction and expression of hemagglutinin (HA) epitope-tagged g5R. The g5R gene and flanking upstream sequence containing the ASFV promoter region were amplified by PCR from clone LMw16 (9) containing Malawi LIL 20/1 isolate DNA, with primers incorporating upstream *Kpn*I (GCGGGTACCTGA ATATCTGTGAACACGGC) and downstream *Bam*HI (GCGGGATCCATGC TTATATCGTAAATAGTTTTTAATAAA) sites. These primers amplify the coding region of g5R without the C-terminal stop codon. This fragment was cloned upstream and fused in frame with a sequence encoding the HA epitope tag in the pcDNA3 vector (Invitrogen) to give plasmid UPg5RHA. This plasmid was transfected into Vero cells which were infected with the ASFV BA71V isolate. At various times postinfection (7, 12, and 16 h) cells were fixed in 4% paraformaldehyde, permeabilized in 0.2% Triton X-100, and stained with rat anti-HA monoclonal antibody (1 in 600 dilution; Roche) and Alexa Fluor 568 goat anti-rat immunoglobulin G conjugate (1 in 800 dilution; Molecular Probes). Cells were visualized with a Leica TCS NT confocal microscope.

Other methods. Protein concentrations were measured by the Coomassie blue dye-binding method (17).

RESULTS AND DISCUSSION

Sequence alignment. An initial BLAST search with the ASFV g5Rp sequence against the GenBank nonredundant database showed it to be most closely related to the mammalian Ap_4A hydrolases, enzymes that cleave Ap_4A (and Gp_4G) asymmetrically to AMP (GMP) and ATP (GTP) but which also have lower activity toward other dinucleoside and nucleoside polyphosphates with four or more phosphate groups. In a gapped alignment, human Ap_4A hydrolase shares 24% overall sequence identity and 33% similarity with g5Rp over the aligned residues. These values increase to 36 and 48%, respectively, over a 56-amino-acid residue section that spans the Nudix motif (Fig. 1). Of particular note is the presence in g5Rp of the conserved tyrosine residue that is found 17 amino acids to the C-terminal side of the Nudix motif in all animal, plant, and prokaryotic asymmetrical Ap_4A hydrolases (10). Thus, it was anticipated that g5Rp might hydrolyze dinucleoside polyphosphates.

Purification and properties of g5Rp. The ASFV g5R ORF was cloned into the pET15b expression vector and expressed in *E. coli*. After incubation with IPTG (isopropyl-β-D-thiogalactopyranoside), a major protein of the expected size (30 kDa) was induced (Fig. 2). The recombinant histidine-tagged protein was purified to near homogeneity by chromatography on Ni^{2+}-NTA-agarose (Fig. 2). When assayed with a wide range of known Nudix hydrolase substrates, it showed no activity with nucleotide sugars, NAD^+, NADH, FAD, or coenzyme A but, as predicted, it hydrolyzed nucleoside and dinucleoside polyphosphates (Fig. 3). However, unlike the typical eukaryotic Ap_4A hydrolases, g5Rp showed a much wider range of substrate utilization, particularly with respect to nucleoside 5′-triphosphates. Thus, when assayed with a fixed concentration of substrate (200 μM), g5Rp showed the highest activity with GTP, followed by adenosine 5′-tetraphosphate (p_4A), adenosine 5′-pentaphosphate (p_5A), and dGTP. The diguanosine nucleotides Gp_3G, Gp_4G, and Gp_5G were also substrates, giving somewhat higher activity than the corresponding diadenosine nucleotides Ap_3A, Ap_4A, and Ap_5A. Heterodinucleotides such as Ap_4G showed intermediate activity, although Ap_2G was inactive as a substrate. Introduction of a 7-methyl group on one or both of the guanosine residues substantially reduced the activity toward the guanine-containing dinucleotides such that the classical cap analogue, $7mGp_3A$, was completely inactive as a substrate (Fig. 3). Since the methylated cap analogues are unstable at a pH higher than 9.0 due to nucleophilic attack on the C-8 position of the imidazole ring (8, 25), assays with these compounds were carried out at pH 8.3 rather than the optimum of pH 9.5 (see below), and the results were adjusted by comparison with the activity toward Gp_4G at pH 8.3.

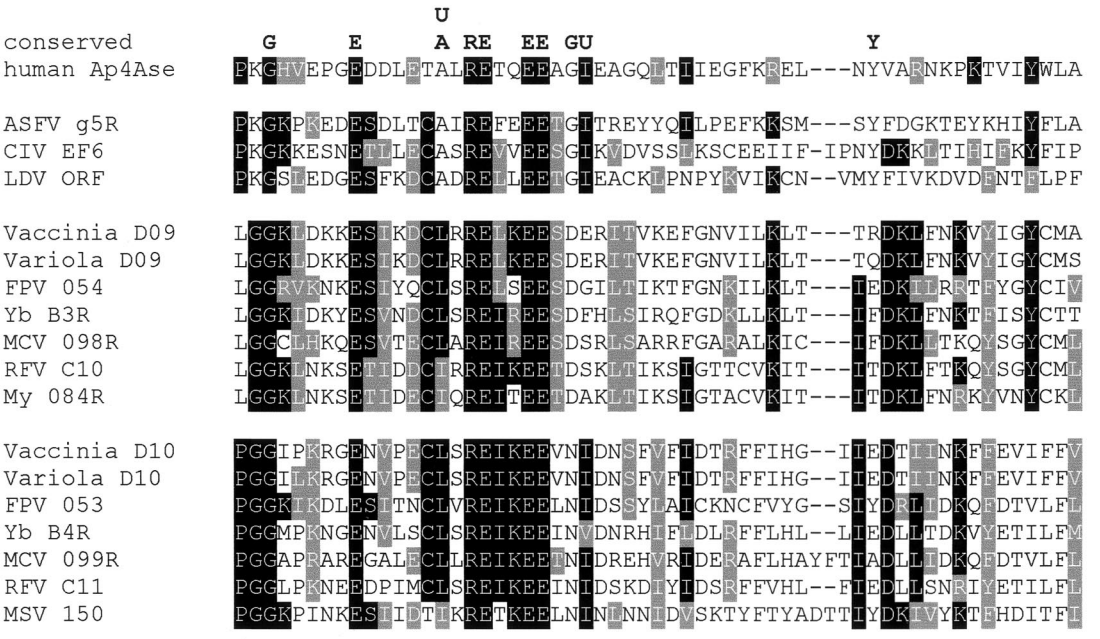

FIG. 1. Partial sequence alignment of the region of virally encoded Nudix hydrolases surrounding the Nudix motif. Alignments were performed with the CLUSTAL X program. Residues that are identical or similar in more than half the sequences are shaded black and gray, respectively. The conserved amino acids of the Nudix motif and the downstream tyrosine residue conserved in Ap_4A hydrolases are shown in boldface above the partial human Ap_4A hydrolase sequence (U is any hydrophobic aliphatic amino acid). Viral sequences are arranged into three groups: the iridovirus and ASFV sequences, followed by the vaccinia virus D9-related sequences, followed by the vaccinia virus D10-related sequences. Abbreviations: Ap4Ase, Ap_4A hydrolase; CIV, Chilo iridescent virus; LDV, lymphocystis disease virus; FPV, fowlpox virus; Yb, Yaba monkey tumor virus; MCV, molluscum contagiosum virus; RFV, rabbit fibroma virus; My, myxoma virus; MSV, Melanoplus sanguinipes entomopoxvirus.

The enzyme had a strict alkaline pH optimum of 9.5; the activity at pH 7.0 was only 5% of that at pH 9.5 (not shown). Several other Nudix hydrolases have markedly alkaline pH optima. A divalent cation was absolutely required with Mn^{2+} at 3 mM supporting 50% higher activity than Mg^{2+} at 10 to 15 mM (not shown).

Products of nucleotide hydrolysis. Analysis of the products of hydrolysis with various substrates indicated that g5Rp can act both as a phosphohydrolase and as a pyrophosphatase. For example, ATP yielded predominantly ADP and P_i (Fig. 4a).

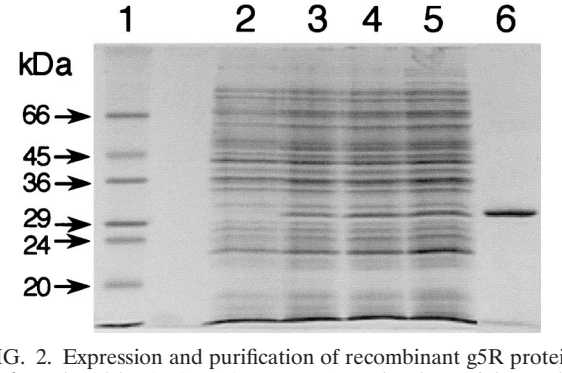

FIG. 2. Expression and purification of recombinant g5R protein in *E. coli* analyzed by SDS-PAGE. Lane 1, molecular weight markers. Samples of soluble protein were extracted from *E. coli* transformed with pET-g5R and induced with 0.5 mM IPTG for 0 h (lane 2), 1 h (lane 3), 2 h (lane 4), and 3 h (lane 5). Lane 6 shows a sample of recombinant g5R protein after purification on Ni^{2+}-NTA-agarose.

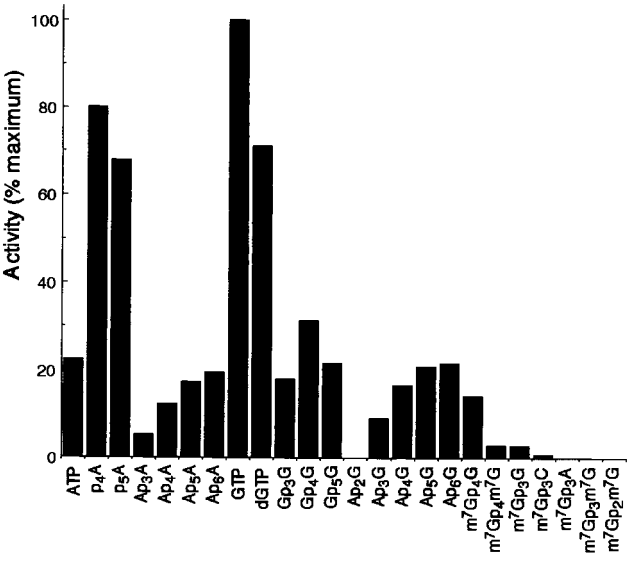

FIG. 3. Nucleotide substrate utilization by g5Rp. Rates of hydrolysis were determined from a 50-μl assay sample by HPLC at a fixed substrate concentration of 200 μM with 2.1 μg of enzyme protein as described in Materials and Methods and are expressed relative to the rate of GTP hydrolysis. The 100% value corresponds to 0.2 μmol/min/mg of protein. Values are the means of duplicate determinations with a difference between each determination and the mean of ≤5%.

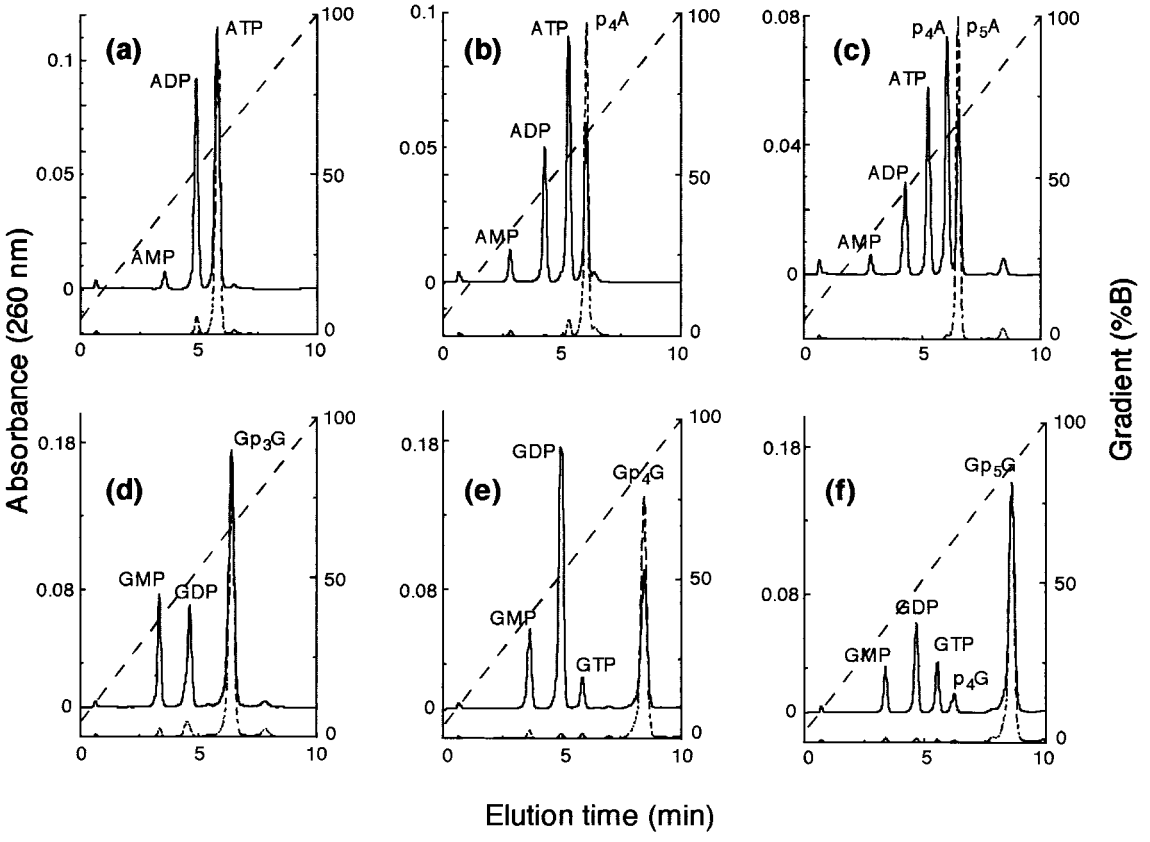

FIG. 4. Identification of the products of hydrolysis of a selection of substrates by g5Rp. Rates of hydrolysis were determined by HPLC at a fixed substrate concentration of 200 μM as described in Materials and Methods. The substrates were ATP (a), p_4A (b), p_5A (c), Gp_3G (d), Gp_4G (e), and Gp_5G (f). The absorbance profiles of control incubations without enzyme are offset by −0.02 for clarity. Curves: with enzyme (solid line), without enzyme (dotted line), and gradient (dashed line).

The small amount of AMP observed appears to come directly from ATP rather than ADP since ADP itself was not a substrate (data not shown). GTP yielded GDP + P_i. Similarly, p_4A and p_5A gave ATP + P_i and p_4A + P_i, respectively, as initial products, with the nucleotide product then acting as a secondary substrate (Fig. 4b and c). With Gp_3G as substrate, the products were GDP and GMP (Fig. 4d). With Gp_4G, the major product was GDP, indicating a predominantly symmetrical mode of attack, with lower amounts of GTP and GMP (Fig. 4e). The GDP could not have all arisen from GTP after initial asymmetrical hydrolysis since it was always in great excess over GMP. Furthermore, it could not have arisen from a contaminating, reversible guanine nucleotide-dependent guanylate kinase activity acting on GTP and GMP since incubation of GDP on its own yielded no GTP or GMP (not shown). The last observation also shows that GTP and GMP are primary products in addition to GDP, so the enzyme must be capable of both symmetrical and asymmetrical hydrolysis by attack at two different phosphate groups in the active site. The excess of GMP over GTP in the products is due to conversion of some of the GTP to GDP + P_i. Two modes of attack are also indicated for Gp_5G hydrolysis by the presence of p_4G and the magnitude of the GDP peak (Fig. 4f). This pattern of alternative hydrolytic attack is very similar to that found with the eukaryotic Ap_6A hydrolases (DIPP), Nudix hydrolases that prefer the higher-order polyphosphates to Ap_4A, Gp_4G, etc., and for which p_4A and p_5A are also good substrates (5, 13, 19). Hydrolysis of Ap_6A by the *Saccharomyces cerevisiae* Ddp1 protein in the presence of $H_2{}^{18}O$ revealed dual sites of attack within the polyphosphate chain (5). Since this flexibility within the active site also extends to a remarkable ability to act as highly efficient phosphohydrolases toward the diphosphoinositol polyphosphates PP-$InsP_5$ and $[PP]_2$-$InsP_4$, these compounds were also tested as substrates for g5Rp.

Activity with diphosphoinositol polyphosphates. Despite an overall low degree of sequence similarity between g5Rp and the DIPP Nudix hydrolases, g5Rp was found to metabolize PP-$InsP_5$ and $[PP]_2$-$InsP_4$. The first-order rate constants for both substrates were similar: k^{-1} (for PP-$InsP_5$) = 2.9 ± 0.8 mg^{-1} min^{-1} (n = 7) and k^{-1} (for $[PP]_2$-$InsP_4$) = 3.1 ± 0.8 mg^{-1} min^{-1} (n = 10). Unlike mammalian DIPP, g5Rp was found to preferentially remove the same β-phosphate from both substrates. DIPP removes the 5-β-phosphate from PP-$InsP_5$ but attacks predominantly the other β-phosphate (tentatively assigned as 6-β-phosphate) from $[PP]_2$-$InsP_4$ to yield 5-PP-$InsP_5$, which is then further metabolized to $InsP_6$ (23, 28). However, the intermediate product of $[PP]_2$-$InsP_4$ metabolism by g5Rp did not cochromatograph with an authentic 5-PP-$InsP_5$ standard, suggesting that it is probably 6-PP-$InsP_5$ (Fig. 5). This was then further slowly metabolized to $InsP_6$. As pre-

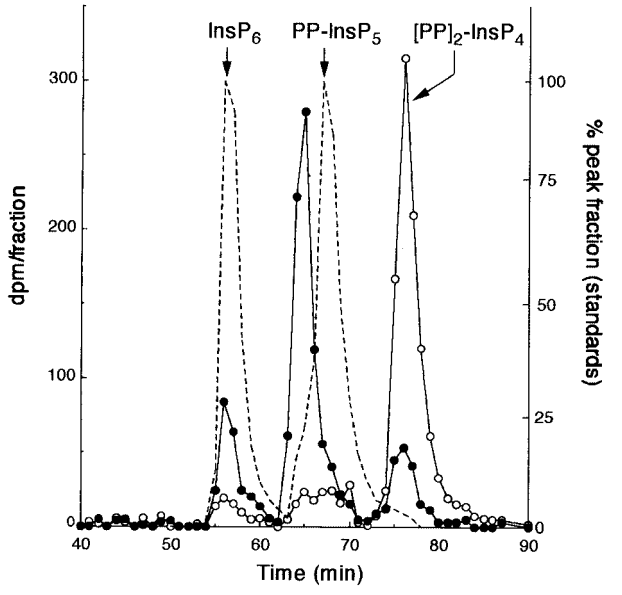

FIG. 5. Activity of g5Rp toward $[PP]_2$-$InsP_4$ in vitro. Activity was measured by incubation of g5Rp with $[^3H][PP]_2$-$InsP_4$ for 30 min and analysis of the products by HPLC as described in Materials and Methods (●). The corresponding HPLC profile from a zero time control is also shown (○), as are the relative elution profiles of authentic $InsP_6$ and 5-PP-$InsP_5$ standards (dotted line).

viously shown for mammalian and fungal members of the DIPP subfamily, 5-PP-$InsP_5$ was quickly converted by g5Rp to $InsP_6$ (not shown), and no further hydrolysis products of $InsP_6$ were observed starting from either PP-$InsP_5$ or $[PP]_2$-$InsP_4$. Thus, in contrast to DIPP, g5Rp appears to preferentially remove the 5-β-phosphate from both PP-$InsP_5$ and $[PP]_2$-$InsP_4$. In this respect, it resembles the unrelated multiple inositol polyphosphate phosphatase (7, 23).

Kinetic parameters. K_m and k_{cat} values were determined for several of the best nucleotide substrates and for PP-$InsP_5$ (Table 1). For the nucleotides, K_m values were all within the range of 0.5 to 4 mM, while the k_{cat} values varied from 0.35 to 0.86 s^{-1}. Comparison of the k_{cat}/K_m ratios confirmed that GTP was the most efficient nucleotide substrate, being ca. 10-fold better than Ap_4A. However, although the k_{cat} value for PP-$InsP_5$ is 5- to 10-fold lower than for the nucleotides (0.076 s^{-1}), the substantially lower K_m of 1.2 μM for PP-$InsP_5$ results in a 60-fold-higher k_{cat}/K_m ratio for this substrate compared to GTP and so allows classification of g5Rp as a novel diphosphoinositol polyphosphate phosphohydrolase on the basis that PP-$InsP_5$ gives the highest k_{cat}/K_m ratio. We were unable to generate more detailed kinetic data for $[PP]_2$-$InsP_4$ hydrolysis due to insufficient amounts of this material. This classification is also consistent with estimated levels of PP-$InsP_5$ in vivo. Given that $InsP_6$ has a typical concentration range of 15 to 100 μM (22) and that PP-$InsP_5$ is ca. 3.5% of the level of $InsP_6$ (Table 2), then PP-$InsP_5$ will be ca. 0.5 to 3.4 μM. The K_m for PP-$InsP_5$ is 1.2 μM. The high K_m values measured for p_4A, p_5A, Ap_4A, and Gp_4G suggest that these are not significant substrates in vivo since these compounds are generally found only in the submicromolar to low micromolar range and the known specific p_4A and Ap_4A hydrolases have K_m values for their substrates within this range (11, 12). On the other hand, the K_m values for ATP and GTP are within the normal concentration ranges of these nucleotides, so it is possible that they, too, may serve as substrates for g5Rp in vivo.

TABLE 1. Kinetic constants[a]

Substrate	K_m[b] (mM)	k_{cat}[b] (s^{-1})	k_{cat}/K_m (10^3 M^{-1} s^{-1})
ATP	0.92	0.37	0.40
p_4A	1.36	0.86	0.63
p_5A	0.58	0.45	0.78
Ap_4A	3.90	0.35	0.09
GTP	0.67	0.67	1.00
Gp_4G	1.70	0.56	0.34
PP-$InsP_5$	0.0012 ± 0.003	0.076 ± 0.009	63.3 ± 9.2

[a] Reaction rates were determined by HPLC as described in Materials and Methods.

[b] K_m and k_{cat} values were determined by hyperbolic regression analysis. Except for PP-$InsP_5$, where $n = 3$ and the standard error of the mean is given, all values quoted are the means of duplicate determinations with a difference between each determination and mean of ≤15%.

TABLE 2. Substrate metabolism during ASFV infection[a]

Metabolite	Mean % ± SEM for:			
	4 h uninfected	4 h + ASFV	20 h uninfected	20 h + ASFV
$InsP_4$	8 ± 1	7 ± 1	8 ± 1	6 ± 1
$InsP_5$	51 ± 1	49 ± 1	53 ± 1	54 ± 1
$InsP_6$	48 ± 1	49 ± 1	46 ± 1	45 ± 1
PP-$InsP_5$	1.6 ± 0.1	1.7 ± 0.1	1.6 ± 0.1	0.9 ± 0.1
$[PP]_2$-$InsP_4$	0.06 ± 0.02	0.07 ± 0.01	0.04 ± 0.02	0.04 ± 0.01
ATP[b]	100	83	100	48
GTP[b]	100	100	100	45

[a] Data are from four to seven determinations and are presented as the mean ± SEM of each inositol phosphate as a percentage of the total radioactivity in $InsP_5$ + $InsP_6$ + PP-$InsP_5$ + $[PP]_2$-$InsP_4$. Levels of $[PP]_2$-$InsP_4$ are at the limit of detection.

[b] ATP and GTP levels are from a single experiment, performed in quadruplicate, and expressed as a percentage of the control values.

Substrate metabolism in ASFV-infected cells. To determine which of the major g5Rp substrates might be affected significantly in vivo during viral infection, Vero cells were labeled with [^{3}H]inositol for 3 days and then infected with ASFV. The intracellular levels of inositol polyphosphate metabolites and of ATP and GTP were then measured 4 and 20 h postinfection. ASFV infection led to reductions in the levels of ATP, GTP, and PP-$InsP_5$ concomitant with the expression of g5Rp, reaching 50% in each case by 20 h postinfection (Table 2). Thus, all three compounds measured may be substrates in vivo. The reduction in PP-$InsP_5$ is unlikely to be simply a consequence of depletion of the ATP pool since previous experiments with DDT_1 MF-2 Syrian hamster vas deferens cells have shown that a 30-min treatment with NaF, which causes a 70% decrease in cellular ATP, doubles the level of PP-$InsP_5$, indicating that the concentration of PP-$InsP_5$ does not merely mirror that of ATP per se (20). This supports a specific role for g5Rp in reducing the intracellular level of PP-$InsP_5$.

Expression and subcellular localization of HA epitope-tagged g5Rp. A fragment of the ASFV genome, containing the g5R gene and a 250-bp upstream promoter region, was amplified by PCR and cloned upstream and in frame with a se-

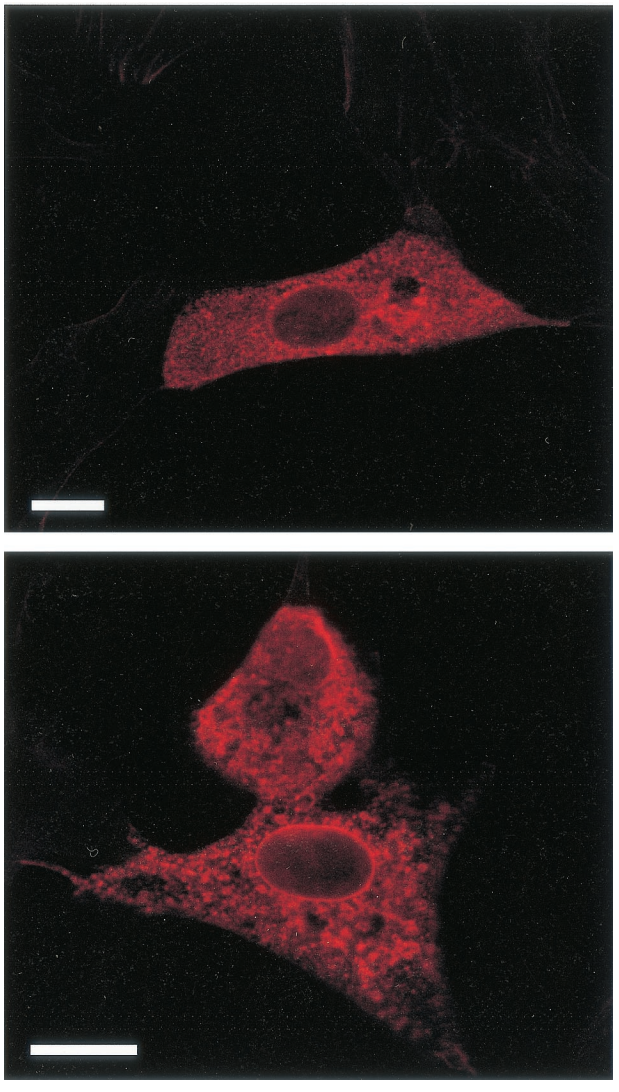

FIG. 6. Localization of an HA epitope-tagged g5R protein in ASFV-infected cells. A plasmid containing the g5R gene fused to a C-terminal sequence encoding the HA epitope tag and expressed under the control of its own ASFV promoter was transfected into Vero cells that were infected with the BA71V isolate of ASFV. Cells were fixed in paraformaldehyde at 10 h postinfection, permeabilized with 0.2% Triton X-100, stained with rat anti-HA monoclonal antibody (1 in 800 dilution) and goat anti-rat Alexa Fluor 568 conjugate secondary antibody (1 in 800 dilution), and then visualized by confocal microscopy. The two panels show different representative cells. Bars, 10 μm.

quence encoding the HA epitope tag. This plasmid was transfected into ASFV-infected Vero cells and at various times postinfection the cells were fixed, permeabilized, stained with rat anti-HA monoclonal antibody and goat anti-rat Alexa Fluor 568 conjugate, and then visualized by confocal microscopy. Expression of the HA epitope-tagged g5R protein was observed from ca. 7 h postinfection and showed a localization typical of rough endoplasmic reticulum (Fig. 6).

Conclusions. The biochemical activity of a virally encoded Nudix hydrolase, the ASFV g5R protein, has been determined for the first time. It is able to hydrolyze a range of guanine and adenine nucleoside and dinucleoside polyphosphates but exhibits highest substrate efficiency with PP-$InsP_5$. Taken together, the facts that (i) the in vitro activity of g5Rp is greatest toward PP-$InsP_5$, (ii) the K_m for PP-$InsP_5$ is close to the known concentration of this compound in vivo, and (iii) the level of PP-$InsP_5$ is reduced after viral infection, all suggest that this may be a physiologically relevant substrate in vivo, although confirmation of this will require measurement of PP-$InsP_5$ levels in cells infected with ASFV from which the g5R gene has been deleted or placed under the control of an inducible promoter. The functional significance of this reduction in PP-$InsP_5$ remains unclear, although we can predict that PP-$InsP_5$-dependent pathways in infected cells may be inhibited. In yeast cells which lack $InsP_6$ kinase and are therefore deficient in PP-$InsP_5$ synthesis, the vacuoles are abnormally small and fragmented, indicating that $InsP_6$ and PP-$InsP_5$ may interact with proteins involved in membrane dynamics (21). ASFV replicates in cytoplasmic factory areas which are rich in membranes. During morphogenesis the virus particle is formed by a process that involves wrapping of the nucleoprotein core in a double membrane layer derived from the endoplasmic reticulum (6, 18). Formation of virus factories and virus morphogenesis requires manipulation of components of the cellular secretory pathway by the virus, and possibly manipulation of the metabolism of PP-$InsP_5$ is important for this process. Transient expression of an HA epitope-tagged g5R protein under control of its own promoter in ASFV-infected cells showed an apparent localization in the rough endoplasmic reticulum. The g5R protein contains neither an obvious signal peptide sequence nor an endoplasmic reticulum retention signal. It is therefore very unlikely that the protein is translocated into the endoplasmic reticulum lumen. Instead, it may be associated with endoplasmic reticulum-resident proteins on the cytosolic side. The reason for this localization of g5R is not clear, but it suggests a localized effect of the enzyme on the metabolism of its substrates.

These proposals for the function of the ASFV g5R protein contrast with what has been suggested for the vaccinia D10 Nudix hydrolase. Overexpression of the D10 gene severely inhibited viral protein synthesis, decreased the steady-state level of late viral mRNA, and blocked the formation of infectious virus (24). However, cap-independent reporter gene expression was not affected. Overexpression of D9 also affected gene expression but to a lesser extent. Based on the knowledge that some Nudix hydrolases degrade cap-like dinucleoside polyphosphates, it was suggested that the D10 protein might bind to or hydrolyze cap structures and so affect the stability or translatability of mRNAs (24). Although we have not measured these aspects of gene expression in our system, the fact that 7-methylation of guanine dinucleotides greatly reduces their ability to act as substrates for g5Rp implies that g5Rp is unlikely to be involved in the turnover of mRNA caps.

Examination of the sequences of the virally encoded Nudix hydrolases suggests that different family members may indeed have different activities. Only ASFV g5Rp and the closely related iridovirus proteins have the tyrosine residue downstream of the Nudix motif in the same position that is conserved in all Ap_4A hydrolases (Fig. 1) (10). This residue is known to stack with one of the two adenine rings in Ap_4A (S. Bailey, J. B. Rafferty, and A. G. McLennan, unpublished data). Although a few individual members of the poxvirus D9 and

D10 subfamilies have tyrosine or phenylalanine at this position, this is not consistent, as would be expected if all D9 and D10 members perform the same function for each poxvirus. Unless a different aromatic residue in the D9 and D10 proteins functionally replaces this conserved tyrosine (e.g., the residue 7 positions from the right hand end of the sequences depicted in Fig. 1), then it is likely that the g5R, D9 and D10 proteins do have enzymatically distinct activities and, therefore, functions. Future comparative analysis of cells infected with poxviruses and ASFV either overexpressing or deleted for these genes, combined with an in vitro analysis of the D9 and D10 proteins, should clarify the situation and lead to a complete understanding of the role of Nudix hydrolases in the infectious cycles of these large DNA viruses.

ACKNOWLEDGMENTS

A.G.M. was financially supported by the Leverhulme Trust, and S.T.S. was supported by The Royal Society and Tenovus-Scotland. E.D. and J.S. were supported by the Polish Committee for Scientific Research (KBN 6 P04A 055 17).

We thank S. R. F. Twigg, H. Schlüter, and J. R. Falck for generously providing materials. We thank P. Monaghan and H. Cook for carrying out the confocal microscopy.

REFERENCES

1. **Bessman, M. J., D. N. Frick, and S. F. O'Handley.** 1996. The MutT proteins or "Nudix" hydrolases, a family of versatile, widely distributed, "housecleaning" enzymes. J. Biol. Chem. **271:**25059–25062.
2. **Caffrey, J. J., S. T. Safrany, X. N. Yang, and S. B. Shears.** 2000. Discovery of molecular and catalytic diversity among human diphosphoinositol-polyphosphate phosphohydrolases: an expanding Nudt family. J. Biol. Chem. **275:** 12730–12736.
3. **Cartwright, J. L., P. Britton, M. F. Minnick, and A. G. McLennan.** 1999. The *ialA* invasion gene of *Bartonella bacilliformis* encodes a (di)nucleoside polyphosphate hydrolase of the MutT motif family and has homologs in other invasive bacteria. Biochem. Biophys. Res. Commun. **256:**474–479.
4. **Cartwright, J. L., L. Gasmi, D. G. Spiller, and A. G. McLennan.** 2000. The *Saccharomyces cerevisiae PCD1* gene encodes a peroxisomal Nudix hydrolase active towards coenzyme A and its derivatives. J. Biol. Chem. **275:**32925–32930.
5. **Cartwright, J. L., and A. G. McLennan.** 1999. The *Saccharomyces cerevisiae* YOR163w gene encodes a diadenosine 5′,5‴-P^1,P^6-hexaphosphate hydrolase member of the MutT motif (Nudix hydrolase) family. J. Biol. Chem. **274:**8604–8610.
6. **Cobbold, C., S. M. Brookes, and T. Wileman.** 2000. Biochemical requirements of virus wrapping by the endoplasmic reticulum: involvement of ATP and endoplasmic reticulum calcium store during envelopment of African swine fever virus. J. Virol. **74:**2151–2160.
7. **Craxton, A., J. J. Caffrey, W. Burkhart, S. T. Safrany, and S. B. Shears.** 1997. Molecular cloning and expression of a rat hepatic multiple inositol polyphosphate phosphatase. Biochem. J. **328:**75–81.
8. **Darzynkiewicz, E., J. Stepinski, S. M. Tahara, R. Stolarski, I. Ekiel, D. Haber, K. Neuvonen, P. Lehikoinen, I. Labadi, and H. Lonnberg.** 1990. Synthesis, conformation and hydrolytic stability of P1,P3-dinucleoside triphosphates related to messenger RNA 5′-cap, and comparative kinetic studies on their nucleoside and nucleoside monophosphate analogs. Nucleosides Nucleotides **9:**599–618.
9. **Dixon, L. K.** 1988. Molecular cloning and restriction enzyme mapping of an African swine fever virus isolate from Malawi. J. Gen. Virol. **69:**1683–1694.
10. **Dunn, C. A., S. F. O'Handley, D. N. Frick, and M. J. Bessman.** 1999. Studies on the ADP-ribose pyrophosphatase subfamily of the Nudix hydrolases and tentative identification of *trgB*, a gene associated with tellurite resistance. J. Biol. Chem. **274:**32318–32324.
11. **Garrison, P. N., and L. D. Barnes.** 1992. Determination of dinucleoside polyphosphates, p. 29–61. *In* A. G. McLennan (ed.), Ap_4A and other dinucleoside polyphosphates. CRC Press, Boca Raton, Fla.
12. **Guranowski, A.** 2000. Specific and nonspecific enzymes involved in the catabolism of mononucleoside and dinucleoside polyphosphates. Pharmacol. Ther. **87:**117–139.
13. **Ingram, S. W., S. A. Stratemann, and L. D. Barnes.** 1999. *Schizosaccharomyces pombe* Aps1, a diadenosine 5′,5‴-P^1,P^6-hexaphosphate hydrolase that is a member of the Nudix (MutT) family of hydrolases: cloning of the gene and characterization of the purified enzyme. Biochemistry **38:**3649–3655.
14. **Koonin, E. V.** 1993. A highly conserved sequence motif defining the family of MutT-related proteins from eubacteria, eukaryotes and viruses. Nucleic Acids Res. **21:**4847.
15. **McLennan, A. G.** 1999. The MutT motif family of nucleotide phosphohydrolases in man and human pathogens. Int. J. Mol. Med. **4:**79–89.
16. **McLennan, A. G., J. L. Cartwright, and L. Gasmi.** 2000. The human NUDT family of nucleotide hydrolases: enzymes of diverse substrate specificity. Adv. Exp. Med. Biol. **486:**115–118.
17. **Peterson, G. L.** 1983. Determination of total protein. Methods Enzymol. **91:**95–119.
18. **Rouiller, I., S. M. Brookes, A. D. Hyatt, M. Windsor, and T. Wileman.** 1998. African swine fever virus is wrapped by the endoplasmic reticulum. J. Virol. **72:**2373–2387.
19. **Safrany, S. T., S. W. Ingram, J. L. Cartwright, J. R. Falck, A. G. McLennan, L. D. Barnes, and S. B. Shears.** 1999. The diadenosine hexaphosphate hydrolases from *Schizosaccharomyces pombe* and *Saccharomyces cerevisiae* are homologues of the human diphosphoinositol polyphosphate phosphohydrolase: overlapping substrate specificities in a MutT-type protein. J. Biol. Chem. **274:**21735–21740.
20. **Safrany, S. T., and S. B. Shears.** 1998. Turnover of bis-diphosphoinositol tetrakisphosphate in a smooth muscle cell line is regulated by β_2-adrenergic receptors through a cAMP-mediated, A-kinase-independent mechanism. EMBO J. **17:**1710–1716.
21. **Saiardi, A., J. J. Caffrey, S. H. Snyder, and S. B. Shears.** 2000. The inositol hexakisphosphate kinase family: catalytic flexibility and function in yeast vacuole biogenesis. J. Biol. Chem. **275:**24686–24692.
22. **Shears, S. B.** 2001. Assessing the omnipotence of inositol hexakisphosphate. Cell. Signal. **13:**151–158.
23. **Shears, S. B., N. Ali, A. Craxton, and M. E. Bembenek.** 1995. Synthesis and metabolism of *bis*-diphosphoinositol tetrakisphosphate *in vitro* and *in vivo*. J. Biol. Chem. **270:**10489–10497.
24. **Shors, T., J. G. Keck, and B. Moss.** 1999. Downregulation of gene expression by the vaccinia virus D10 protein. J. Virol. **73:**791–796.
25. **Stepinski, J., M. Bretner, M. Jankowska, K. Felczak, R. Stolarski, Z. Wieczorek, A. L. Cai, R. E. Rhoads, A. Temeriusz, D. Haber, and E. Darzynkiewicz.** 1995. Synthesis and properties of p(1),p(2)-, p(1),p(3)-, and p(1),p(4)-, dinucleoside di-, tri-, and tetraphosphate mRNA 5′-cap analogues. Nucleosides Nucleotides **14:**717–721.
26. **Twigg, S. R. F.** 1995. Ph.D. thesis. University of Oxford, Oxford, United Kingdom.
27. **Xu, W. L., C. A. Dunn, and M. J. Bessman.** 2000. Cloning and characterization of the NADH pyrophosphatases from *Caenorhabditis elegans* and *Saccharomyces cerevisiae*, members of a Nudix hydrolase subfamily. Biochem. Biophys. Res. Commun. **273:**753–758.
28. **Yang, X. N., S. T. Safrany, and S. B. Shears.** 1999. Site-directed mutagenesis of diphosphoinositol polyphosphate phosphohydrolase, a dual specificity NUDT enzyme that attacks diadenosine polyphosphates and diphosphoinositol polyphosphates. J. Biol. Chem. **274:**35434–35440.